Dark Population Transfer Mechanism for Sterile Neutrino Dark Matter

George M. Fuller, 1,* Lukáš Gráf, 1,2,† Amol V. Patwardhan, 3,4,‡ and Jacob Spisak, 4 amol V. Patwardhan, 3,4,‡ ¹Department of Physics, University of California, San Diego, La Jolla, California 92093-0319, USA ²Department of Physics, University of California, Berkeley, California 94720, USA ³SLAC National Accelerator Laboratory, 2575 Sand Hill Road, Menlo Park, California 94025, USA ⁴School of Physics and Astronomy, University of Minnesota, Minneapolis, Minnesota 55455, USA ⁵Max-Planck-Institut für Kernphysik, 69117 Heidelberg, Germany



(Received 4 March 2024; revised 27 June 2024; accepted 23 September 2024; published 29 October 2024)

We present a mechanism for producing a cosmologically significant relic density of one or more sterile neutrinos. This scheme invokes two steps: First, a population of "heavy" sterile neutrinos is created by scattering-induced decoherence of active neutrinos. Second, this population is transferred, via sterile neutrino self-interaction-mediated scatterings and decays, to one or more lighter mass (~10 keV to ~1 GeV) sterile neutrinos that are far more weakly (or not at all) mixed with active species and could constitute dark matter. Dark matter produced this way can evade current electromagnetic and structurebased bounds, but may nevertheless be probed by future observations.

DOI: 10.1103/PhysRevLett.133.181002

Introduction—An outstanding issue at the heart of physics and astronomy is the identity of dark matter (DM). Among the many beyond-standard-model (BSM) candidates for DM, the neutrino sector offers an alluring possibility: a standard model (SM) singlet "sterile" neutrino. However, the simplest mechanisms for producing a dark matter-relevant relic density of these particles are challenged by x-ray and large scale structure observations (e.g., [1-10] and references therein). In this Letter we propose a mechanism for producing a relic density of sterile neutrinos that may be able to evade current bounds, yet may be probed by future observations.

The standard Dodelson-Widrow mechanism [11] for sterile neutrino dark matter production requires only a vacuum mixing between the sterile and active (SM) neutrinos. At ultrahigh temperatures in the early Universe, this mixing is medium suppressed, but subsequently, at lower temperatures, $T \sim \text{GeV}$, a cosmologically significant abundance of sterile neutrinos can be built up via active neutrino scattering-induced decoherence. However, the same mixing that enables this freeze-in production scenario also provides a sterile neutrino radiative decay channel into a photon and an active neutrino [12]. Demanding a relic density of a

*Contact author: gfuller@physics.ucsd.edu [†]Contact author: lukas.graf@berkeley.edu [‡]Contact author: apatward@umn.edu Contact author: jspisak@ucsd.edu

Published by the American Physical Society under the terms of the Creative Commons Attribution 4.0 International license. Further distribution of this work must maintain attribution to the author(s) and the published article's title, journal citation, and DOI. Funded by SCOAP³.

long-lived DM candidate in this scheme picks out a $m_{\rm s} \sim {\rm keV}$ mass scale associated with the sterile state. That implies a decay-generated x-ray line at an energy $E_{\rm y} = m_{\rm s}/2$ that is nicely matched to the energy sensitivity range of the x-ray observatories, enabling them to provide stringent constraints [2].

Other production mechanisms for sterile neutrino DM abound, but all require additional new physics on top of the minimalist mass and vacuum mixing parameters of Dodelson-Widrow. Some propose the sterile neutrino DM abundance to stem from decays of heavier particles, e.g., scalars [9,13–18], other sterile neutrinos [19,20], or primordial black holes [21], while being relatively agnostic about the active-sterile coupling. Similarly, the correct sterile neutrino population can be achieved via thermalization [22], dilution of their initially produced overabundance [23], or, e.g., via strongly interacting massive particle (SIMP)-like freeze-out [24]. Other production scenarios focus on altering the active-sterile mixing. One example is the Shi-Fuller mechanism [1,25–30] wherein the inmedium active-sterile mixing is resonantly enhanced by a cosmic lepton number asymmetry, which may be generated through the asymmetric decay of heavier sterile states (à la ν MSM: e.g., [13,31–34] and many more). Another invokes mixing parameters mediated by scalar [35-37] or axionlike [38] fields, or a dark photon [39].

Intriguing dynamics can be achieved by bringing selfinteractions into the picture. Strongly self-interacting active neutrinos can boost sterile neutrino production and, hence, result in the required DM relic abundance at smaller mixing angles [40,41]. On the other hand, self-interactions among the sterile neutrinos themselves can lead to resonantly enhanced production, which has been investigated in both the heavy mediator [42] and light mediator limits [43,44]. These considerations lead us to a scheme that utilizes the advantages of both active neutrino scattering-induced decoherence and sterile neutrino self-interactions. Though there could be many sterile states, in a dark sector for example [45], we can illustrate the key features of our mechanism by considering sterile neutrino DM production in the presence of two sterile species with a dark self-interaction channel. This simple scenario may be further motivated by the experimental observations requiring at least two nonzero active neutrino masses.

Dark sector dynamics—The basic idea of this mechanism is the following: (i) The heavier of the two sterile neutrinos has a small mixing with active neutrinos, enabling scattering-induced decoherence to populate this heavier sterile state. (ii) Before the heavy sterile neutrino population can decay back into the SM by virtue of its mixing, self-interactions within the sterile sector engender a population transfer to the lighter sterile neutrino state. (iii) The population of the lighter sterile state (or states) created this way persists until the present and can be the dark matter or a component of it, provided its mixing with the active neutrinos is sufficiently small.

The background evolution of the SM plasma and the dark sector are governed by the following set of equations:

$$\frac{\mathrm{d}\rho_{\mathrm{SM}}}{\mathrm{d}t} = -3H(\rho_{\mathrm{SM}} + P_{\mathrm{SM}}) - \frac{\mathrm{d}\rho_{\mathrm{inj}}}{\mathrm{d}t},\tag{1}$$

$$\frac{\mathrm{d}\rho_{\mathrm{DS}}}{\mathrm{d}t} = -3H(\rho_{\mathrm{DS}} + P_{\mathrm{DS}}) + \frac{\mathrm{d}\rho_{\mathrm{inj}}}{\mathrm{d}t},\tag{2}$$

$$H^{2} = \frac{8\pi G}{3}(\rho_{\rm SM} + \rho_{\rm DS}),\tag{3}$$

where $\rho_{\rm SM/DS}$ and $P_{\rm SM/DS}$ are the energy density and pressure in the SM plasma and dark sector, respectively, and H is the Hubble parameter. The first two equations describe energy conservation within each sector, with the exception of a small amount of energy transfer $\mathrm{d}\rho_{\rm inj}/\mathrm{d}t$ from the SM plasma into the dark sector. The last equation is simply the Friedmann equation in a flat universe.

The energy injected into the dark sector via scattering-induced decoherence is [1]

$$\frac{\mathrm{d}\rho_{\rm inj}}{\mathrm{d}t} = \int \frac{\mathrm{d}^3 p}{(2\pi)^3} E f_{\nu_\alpha}^{\rm (eq)} \frac{\Gamma_\alpha}{2} P(\nu_\alpha \to N_1), \tag{4}$$

where $P(\nu_{\alpha} \to N_1)$ is the probability that an active neutrino of flavor $\alpha = e, \mu$, or τ , energy E, and momentum p has converted into N_1 , the heavier sterile neutrino. It depends on the mixing between N_1 and ν_{α} ; here we will assume that the mixing occurs only with one flavor, characterized by a single vacuum mixing angle θ . While in our calculations we treat the active-sterile mixing as a free parameter, it nevertheless arises in specific models, e.g., seesaw mass models [46,47].

The scattering rate of an active neutrino on the SM plasma with a temperature $T_{\rm SM}$ is

$$\Gamma_{\alpha}(p, T_{SM}) = C_{\alpha}(p, T_{SM})G_F^2 p T_{SM}^4,$$
 (5)

where $C_{\alpha}(p,T_{\rm SM})$ is a temperature-dependent coefficient and G_F is the Fermi coupling constant. Assuming that the SM neutrinos follow a thermal Fermi-Dirac energy distribution with zero chemical potential for $T_{\rm SM}\gg 1$ MeV, one has $f_{\nu_{\alpha}}^{\rm (eq)}(E,T_{\rm SM})=(e^{E/T_{\rm SM}}+1)^{-1}$. We ignore Pauliblocking effects and the conversion of sterile neutrinos back into active neutrinos, thereby decoupling the energy injection rate from the dynamics within the dark sector. See the Supplemental Material [48] for additional details.

In general, the evolution of the sterile neutrinos is described by a set of coupled Boltzmann equations. However, if we restrict ourselves to the regime where the dark sector quickly reaches thermal equilibrium with itself as a result of self-interactions, then the dark sector's energy density and pressure are completely determined by its temperature, $T_{\rm DS}$, and the masses of the dark sector constituents. This eliminates the need to evolve the individual Boltzmann equations, and Eqs. (1)–(4) form a set of coupled equations for $T_{\rm DS}$, $T_{\rm SM}$, and the scale factor as functions of time. To good approximation, the latter two quantities can be solved for independently of $T_{\rm DS}$, since the energy injected into the dark sector is relatively small. To solve for $T_{\rm DS}$, we numerically evolve Eq. (2) from a starting plasma temperature $T_{\rm SM}$ at which scattering-induced decoherence is highly suppressed, with zero initial abundance for both sterile states.

To demonstrate how the mechanism could work, we choose the dark sector to consist of two sterile neutrinos N_1 (heavy) and N_2 (light) with a scalar mediator ϕ :

$$\mathcal{L} \supset \frac{g_{\phi}^{ij}}{2} \bar{N}_{j}^{C} N_{i} \phi + \text{H.c.}, \tag{6}$$

where i, j = 1, 2. For simplicity, we take all $g_{\phi}^{ij} = g_{\phi}$ to be equal, and take the heavy-mediator limit wherein $G_{\phi} \equiv g_{\phi}^2/m_{\phi}^2$ is the effective interaction strength. Note that taking this limit makes the whole discussion quite general, as it allows us to be agnostic about the specific UV origin of the self-interaction. The scalar ϕ could, in principle, mix with the SM Higgs, providing an additional channel for sterile neutrino production (via scalar decays), e.g., [9,13–15], and complicating the calculation of the relic abundance. Here, for simplicity, we assume that the scalar resides entirely within the dark sector, and has no mixing with the Higgs.

Thermal equilibrium and population transfer within the dark sector may be achieved through various combinations of self-interaction processes, namely, two-to-two scatterings, one-to-three decays, and potentially two-to-four scatterings. These rates scale as follows (see the Supplemental Material

[48] for a more detailed discussion):

$$\Gamma_{\phi,2\to2} \propto \beta G_{\phi}^2 p T^4,$$
 (7)

$$\Gamma_{\phi,1\to3} \propto G_{\phi}^2 m_N^5 / \gamma(p),$$
 (8)

$$\Gamma_{\phi,2\to4} \propto G_{\phi}^2 T^4 \Gamma_{\phi,2\to2}.$$
 (9)

Here, T and β are the temperature and a suppression factor, respectively, parametrizing a Fermi-Dirac-like distribution for the sterile neutrino(s): $f(E,T) \simeq \beta/(e^{E/T}+1)$. $\Gamma_{\phi,X\to Y}$ refers to a ϕ -mediated process with X sterile neutrinos in the initial state and Y sterile neutrinos in the final state. $\gamma(p)$ in Eq. (8) is the Lorentz factor for a heavy sterile neutrino with momentum p, accounting for a time dilation of its lifetime.

These may be evaluated in two regimes of interest: without and with dark sector internal thermalization. Without thermalization, a suppressed Fermi-Dirac form with $T=T_{\rm SM}$ and $\beta\ll 1$ is a reasonable approximation to the N_1 distribution generated by active neutrino scattering-induced decoherence. Subsequently, if the dark sector internally thermalizes, the distribution functions instead assume unsupressed Fermi-Dirac forms (i.e., with $\beta=1$) parametrized by a dark sector temperature $T_{\rm DS}$. Assuming an empty dark sector to begin with, and subsequent energy conservation within the dark sector as it thermalizes, one must have

$$g_{\rm DS}^{\star} T_{\rm DS}^4 = g_{N_1}^{\star} \beta T_{\rm SM}^4, \tag{10}$$

and therefore $T_{\rm DS} < T_{\rm SM}$. Here, $g_{N_1}^{\star}$ and $g_{\rm DS}^{\star}$ are respectively the number of degrees of freedom of the heavy sterile N_1 , and in the dark sector overall. For a typical momentum $p \simeq 3T$, $\Gamma_{\phi,2\to2}$ and $\Gamma_{\phi,2\to4}$ are proportional to T^5 and T^9 , respectively. Therefore, the decrease in temperature from $T_{\rm SM}$ to $T_{\rm DS}$ outweighs the increase of β from $\ll 1$ to $\beta=1$, leading to an overall reduction in the rates postthermalization. The decay rate for the heavy sterile neutrino in the plasma rest frame is always larger after dark sector thermalization because $T_{\rm DS} < T_{\rm SM}$.

To assess the prospects of dark sector internal thermalization, these rates may be compared to the Hubble rate, $H=\sqrt{8\pi g_{\rm SM}^{\star}/3}(T^2/m_{\rm pl})$, where $g_{\rm SM}^{\star}$ is the number of relativistic degrees of freedom in the SM plasma. On the other hand, to avoid resonant overproduction due to the additional in-medium potential provided by the self-interaction, we require that $\Gamma_{\phi,2\to2}<\Gamma_{\alpha}$ [42]. We also require that $g_{\phi}<1$ to stay in the perturbative regime. These requirements may be simultaneously satisfied over some range of G_{ϕ} values, given a sterile neutrino mass m_{N_1} and vacuum mixing angle θ .

This mechanism is illustrated for a particular choice of parameters in Fig. 1. For both $\Gamma_{\phi,2\to2}$ and $\Gamma_{\phi,2\to4}$, the upper

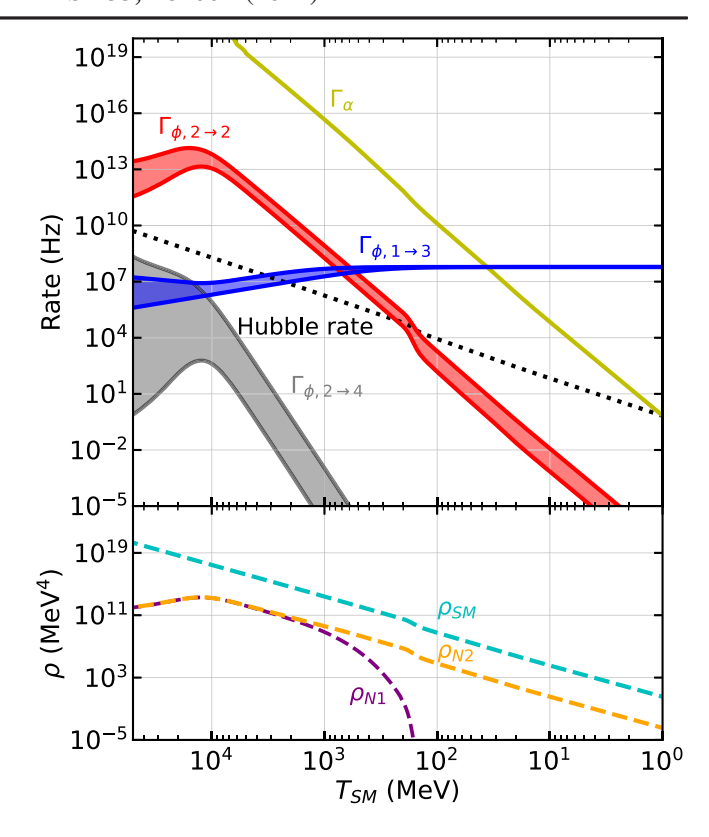


FIG. 1. Bottom: evolution of SM and sterile neutrino energy densities as a function of SM plasma temperature $T_{\rm SM}$. In this scenario, thermalization within the dark sector, and population transfer from the heavier (N_1) to the lighter (N_2) sterile neutrino, are achieved through contemporaneous two-to-two scatterings and one-to-three decays. Top: rates of various processes [Eqs. (3), (5), and (7)–(9)] as indicated. The width of the colored bands represents the variation of the rates as the dark sector thermalizes (see text for details). Here, $m_{N_1}=1$ GeV, $\sin^2(2\theta)=10^{-15}$, $G_{\phi}=0.1G_F$, $\alpha=$ electron, and all rates are evaluated at p=3T.

and lower edges of each band reflect the rate expressions without and with dark sector internal thermalization, respectively. For $\Gamma_{\phi,1\to3}$ the situation is reversed. N_1 is produced via scattering-induced decoherence, and initially the dark sector has not achieved internal thermal equilibrium due to a lack of number-changing processes. This changes once $\Gamma_{\phi,1\to3} > H$: this process increases the number of sterile neutrinos, and the two-to-two processes, which are initially much faster than the decays, ensure the N_1 and N_2 populations equilibrate with roughly equal number densities. Note that SM decay branches for N_1 are subdominant for these parameter choices compared to the dark decays (see Supplemental Material). As the dark sector thermalizes, the rates switch to the opposite sides of the bands [55]. Eventually, N_1 becomes nonrelativistic and is Boltzmann suppressed, transferring N_1 into N_2 . Oneto-three decays, which eventually become faster than twoto-two processes, further aid this transfer. N_2 then persists until the present day as a component of dark matter. Note that the effective mixing between $\nu \leftrightarrow N_2$ arising via loop

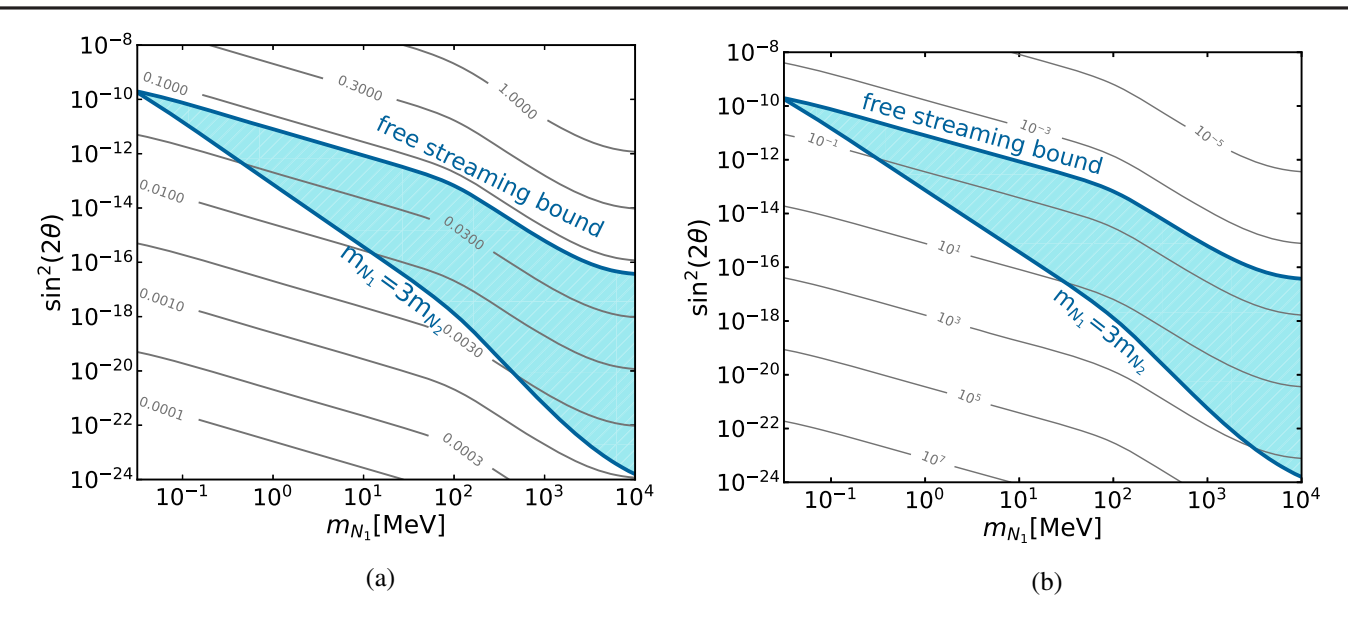


FIG. 2. Across a parameter space of the heavy sterile neutrino rest mass (m_{N_1}) and its mixing angle with the active neutrinos $[\sin^2(2\theta)]$, the following contours are shown. Left: the ratio of the dark sector temperature to the standard model temperature, i.e., $T_{\rm DS}/T_{\rm SM}$, stemming from the energy injected into the dark sector from scattering-induced decoherence, under the assumption that the dark sector thermalizes with itself. The blue region is where all observational and theoretical bounds are satisfied. Right: the mass of N_2 (in MeV) required to account for all of the dark matter in this scenario.

interactions is suppressed relative to $\nu \leftrightarrow N_1$ by a factor of $\sim G_\phi^2 T^4$ at high temperatures due to the additional vertices and internal propagators, and further suppressed by mass threshold effects at lower temperatures.

An alternative scenario can achieve this dark sector internal thermalization through two-to-four processes. Although these are relevant only at high temperatures and for a much smaller slice of the parameter space than the previous example, they would allow for smaller N_1 masses. This is because $\Gamma_{\phi,1\to3} \propto N_1^5$, and so smaller masses have a lower one-to-three rate that may not be significant at high enough $T_{\rm SM}$ to overlap with two-to-two processes.

Parameter space—Under the assumption that the dark sector thermalizes internally, the parameter space in which all of the dark matter is produced is shown in Fig. 2. The left panel shows contours of the final dark sector temperature relative to the SM temperature. In the viable parameter space this ratio is less than one for two reasons: the active-sterile mixing is too small to thermalize the dark sector with the SM, and the SM plasma is heated by the disappearance of relativistic degrees of freedom as the temperature drops. The right panel of Fig. 2 shows contours of the required mass m_{N_2} necessary to make all of the dark matter, given the dark sector temperatures shown in the left panel. It is assumed that the N_1 relic population is converted to N_2 via two-to-two scattering, although the results do not qualitatively change as long as the number density is roughly preserved, e.g., if one-to-three decays occur instead.

The lower boundary on the colored region in the parameter space shown in Fig. 2 comes from the condition that N_1 have a large enough mass to decay into three N_2 , i.e. $m_{N_1} > 3m_{N_2}$, which is the regime we restrict ourselves to in this Letter. The upper boundary of the color region follows from dark matter free streaming considerations, explained below. We choose the upper limit of the N_1 mass range in Fig. 2 to be 10 GeV so that $T_{\rm SM} \gg m_{N_1}$ during the scattering-induced decoherence production period, ensuring N_1 is produced relativistically.

Discussion—A key feature of this mechanism is that it allows for a larger sterile neutrino dark matter mass. Normally, the mass of the sterile neutrino is bounded from above by the requirement that the dark matter does not decay too fast via its active-sterile mixing. In the proposed mechanism, however, the mixing angle of the dark matter candidate sterile neutrino does not affect its relic abundance, and can therefore be arbitrarily small. On the flip side, this mechanism provides discovery potential for current and future x-ray and γ -ray missions across a much wider range of sterile neutrino masses and mixings. Depending on the mass of N_1 , the dark matter mass m_{N_2} in our mechanism can range from ~10 keV-3 GeV. Many x-ray telescopes have explored some of this parameter space (e.g., [56–65]), which will be further probed by the upcoming telescopes ATHENA [66] and XRISM [67]. This also motivates searches for dark matter lines at higher energies, beyond the typical range for sterile neutrino dark matter, using telescopes such as NuSTAR [68-73], HEX-P [74], Fermi-GBM [75], and INTEGRAL-SPI [76,77]. Moreover, heavier N_2 masses allow for decay channels involving additional particles such as electrons, muons, and pions [78], which may generate a more complicated electromagnetic signature than a narrow line.

On the opposite end, the lower bound on the sterile neutrino DM mass is set by the requirement that free-streaming dark matter should not wash out small-scale structure, that is, its average kinetic energy must not be too large. Since dark sector internal thermalization ensures $T_{\rm DS} < T_{\rm SM}$, the sterile neutrino average energy can be considerably lower than in a purely scattering-induced decoherence scenario, resulting in a weaker lower mass bound. The current bound for thermal fermionic dark matter with two degrees of freedom is 9.7 keV at 95% C.L. [79]. For comparison, the corresponding bound for the Dodelson-Widrow scenario can be as strong as 92 keV [10].

The heavy sterile neutrino may in principle be detected in laboratory searches, but unfortunately the mixing angles shown in Fig. 2 are too small for any current or upcoming experiments to detect, see Ref. [80] for a review. (If the scalar mixes with the Higgs it may generate collider signatures of its own [81].) Furthermore, many of these sterile neutrino laboratory searches rely on detecting the sterile neutrino's SM decay products, which would not be effective in the scenario considered here. If, however, decays into SM products dominate over the dark decay branch, larger mixing angles would be required to produce the observed relic abundance. This could potentially allow for detection in experiments close to the preferred parameter space shown in Fig. 2, such as HUNTER [82] and TRISTAN [83-85]. Such scenarios could have significant implications for neutrino decoupling and big-bang nucleosynthesis (BBN) [78,86–89], pre-BBN cosmology [41,90– 92], as well as energy transport in core-collapse supernovae [93–96]. The lighter sterile neutrino N_2 , if it also mixes with the active neutrinos, could be resonantly produced in a supernova core, affecting the explosion dynamics [97–101].

Future work could explore variations to the mechanism. References [19] and [20] discuss dark matter production via energy transfer between multiple sterile neutrinos in the context of a Majoron model and a pseudo-Dirac model with a dark photon, respectively. A lighter dark sector mediator would result in more complicated dynamics, and in certain regions of parameter space can produce the correct relic abundance with just one sterile neutrino [43,44], reproduce the regimes preferred by scenarios of self-interacting dark matter [102-107] which address small structure problems [108–110], or cause dips in the diffuse supernova neutrino background [111]. The decay of a single heavy sterile neutrino into many lighter sterile neutrinos (corresponding, for example, to a tower of massive Kaluza-Klein modes [45] or other rich dark sectors) may lead to an arbitrarily cold dark matter spectrum for arbitrarily large $g_{\rm DS}^{\star}$, see Eq. (10). Such a scenario also would potentially provide a multitude of targets for future electromagnetic searches. We conclude that the future of this dark subject could be bright.

Acknowledgments—The authors would like to thank Kev Abazajian, Chad Kishimoto, Richard Rothschild, and Anna Suliga for fruitful discussions, and Alex Kusenko for helpful comments on the manuscript. This work was supported in part by National Science Foundation (NSF) Grant No. PHY-2209578 at UCSD, the Network for Neutrinos, Nuclear Astrophysics, and Symmetries (N3AS), funded by NSF Grants No. PHY-2020275 and No. PHY-1630782, and the Heising-Simons Foundation, Grant No. 2017-228. A. V. P. would like to acknowledge support from the U.S. Department of Energy (DOE) under Contract No. DE-AC02-76SF00515 at SLAC National Accelerator Laboratory and DOE Grant No. DE-FG02-87ER40328 at the University of Minnesota. J. S. acknowledges support from the UCSD Academic Senate and the UC-LANL SoCal Hub. We would also like to acknowledge the Kavli Institute for Theoretical Physics (NSF Grants No. PHY-1748958 and No. PHY-2309135), the Institute for Nuclear Theory (DOE Grant No. DE-FG02-00ER41132), and the Mainz Institute for Theoretical Physics (MITP), Cluster of Excellence PRISMA+ (Project ID 39083149).

^[1] K. Abazajian, G. M. Fuller, and M. Patel, Phys. Rev. D **64**, 023501 (2001).

^[2] K. Abazajian, G. M. Fuller, and W. H. Tucker, Astrophys. J. **562**, 593 (2001).

^[3] A. D. Dolgov and S. H. Hansen, Astropart. Phys. 16, 339 (2002).

^[4] A. Kusenko, Phys. Rep. 481, 1 (2009).

^[5] K. Abazajian, arXiv:0903.2040.

^[6] R. Adhikari et al., J. Cosmol. Astropart. Phys. 01 (2017) 025.

^[7] A. Boyarsky, M. Drewes, T. Lasserre, S. Mertens, and O. Ruchayskiy, Prog. Part. Nucl. Phys. 104, 1 (2019).

^[8] B. Dasgupta and J. Kopp, Phys. Rep. 928, 1 (2021).

^[9] K. N. Abazajian and A. Kusenko, Phys. Rev. D 100, 103513 (2019).

^[10] I. A. Zelko, T. Treu, K. N. Abazajian, D. Gilman, A. J. Benson, S. Birrer, A. M. Nierenberg, and A. Kusenko, Phys. Rev. Lett. 129, 191301 (2022).

^[11] S. Dodelson and L. M. Widrow, Phys. Rev. Lett. **72**, 17 (1994).

^[12] P. B. Pal and L. Wolfenstein, Phys. Rev. D 25, 766 (1982).

^[13] M. Shaposhnikov and I. Tkachev, Phys. Lett. B 639, 414 (2006).

^[14] A. Kusenko, Phys. Rev. Lett. 97, 241301 (2006).

^[15] K. Petraki and A. Kusenko, Phys. Rev. D 77, 065014 (2008).

^[16] A. Merle, V. Niro, and D. Schmidt, J. Cosmol. Astropart. Phys. 03 (2014) 028.

^[17] B. Shuve and I. Yavin, Phys. Rev. D 89, 113004 (2014).

^[18] A. Abada, G. Arcadi, M. Lucente, G. Piazza, and S. Rosauro-Alcaraz, J. High Energy Phys. 11 (2023) 180.

- [19] G. Alonso-Álvarez and J. M. Cline, Phys. Lett. B 833, 137278 (2022).
- [20] W. Chao, S. Jiang, Z.-Y. Wang, and Y.-F. Zhou, arXiv:2112.14527.
- [21] M. Chen, G.B. Gelmini, P. Lu, and V. Takhistov, J. Cosmol. Astropart. Phys. 07 (2024) 059.
- [22] R. S. L. Hansen and S. Vogl, Phys. Rev. Lett. 119, 251305 (2017).
- [23] A. V. Patwardhan, G. M. Fuller, C. T. Kishimoto, and A. Kusenko, Phys. Rev. D 92, 103509 (2015).
- [24] J. Herms, A. Ibarra, and T. Toma, J. Cosmol. Astropart. Phys. 06 (2018) 036.
- [25] X.-D. Shi and G. M. Fuller, Phys. Rev. Lett. **82**, 2832 (1999).
- [26] C. T. Kishimoto, G. M. Fuller, and C. J. Smith, Phys. Rev. Lett. 97, 141301 (2006).
- [27] C. T. Kishimoto and G. M. Fuller, Phys. Rev. D 78, 023524 (2008).
- [28] J. Ghiglieri and M. Laine, J. High Energy Phys. 11 (2015) 171.
- [29] T. Venumadhav, F.-Y. Cyr-Racine, K. N. Abazajian, and C. M. Hirata, Phys. Rev. D 94, 043515 (2016).
- [30] E. L. Horner, F. Munguia Wulftange, I. A. Ianora, and C. T. Kishimoto, Phys. Rev. D 108, 083503 (2023).
- [31] T. Asaka, S. Blanchet, and M. Shaposhnikov, Phys. Lett. B **631**, 151 (2005).
- [32] T. Asaka and M. Shaposhnikov, Phys. Lett. B 620, 17 (2005).
- [33] T. Asaka, M. Shaposhnikov, and A. Kusenko, Phys. Lett. B 638, 401 (2006).
- [34] M. Shaposhnikov, J. High Energy Phys. 08 (2008) 008.
- [35] F. Bezrukov, A. Chudaykin, and D. Gorbunov, J. Cosmol. Astropart. Phys. 06 (2017) 051.
- [36] F. Bezrukov, A. Chudaykin, and D. Gorbunov, Phys. Rev. D 99, 083507 (2019).
- [37] F. Bezrukov, A. Chudaykin, and D. Gorbunov, Phys. Rev. D 101, 103516 (2020).
- [38] A. Berlin and D. Hooper, Phys. Rev. D **95**, 075017 (2017).
- [39] G. Alonso-Álvarez and J. M. Cline, J. Cosmol. Astropart. Phys. 10 (2021) 041.
- [40] A. de Gouvêa, M. Sen, W. Tangarife, and Y. Zhang, Phys. Rev. Lett. 124, 081802 (2020).
- [41] C. Chichiri, G. B. Gelmini, P. Lu, and V. Takhistov, J. Cosmol. Astropart. Phys. 09 (2022) 036.
- [42] L. Johns and G.M. Fuller, Phys. Rev. D **100**, 023533 (2019).
- [43] T. Bringmann, P. F. Depta, M. Hufnagel, J. Kersten, J. T. Ruderman, and K. Schmidt-Hoberg, Phys. Rev. D 107, L071702 (2023).
- [44] M.D. Astros and S. Vogl, J. High Energy Phys. 03 (2024) 032.
- [45] K. N. Abazajian, G. M. Fuller, and M. Patel, Phys. Rev. Lett. **90**, 061301 (2003).
- [46] A. de Gouvêa, Annu. Rev. Nucl. Part. Sci. **66**, 197 (2016).
- [47] Y. Cai, J. Herrero-García, M. A. Schmidt, A. Vicente, and R. R. Volkas, Front. Phys. 5, 63 (2017).
- [48] See Supplemental Material at http://link.aps.org/supplemental/10.1103/PhysRevLett.133.181002, which

- includes Refs. [49–54], for details regarding the scattering-induced decoherence calculation and sterile neutrino interaction rates.
- [49] T. Asaka, M. Laine, and M. Shaposhnikov, J. High Energy Phys. 01 (2007) 091; 02 (2015) 28.
- [50] J. Ghiglieri and M. Laine, J. Cosmol. Astropart. Phys. 07 (2016) 015.
- [51] D. Notzold and G. Raffelt, Nucl. Phys. **B307**, 924 (1988).
- [52] C. Quimbay and S. Vargas-Castrillón, Nucl. Phys. **B451**, 265 (1995).
- [53] V. Barger, R. J. N. Phillips, and S. Sarkar, Phys. Lett. B 352, 365 (1995).
- [54] F. F. Deppisch, W. Liu, and M. Mitra, J. High Energy Phys. 08 (2018) 181.
- [55] Unless a freeze-out ($\Gamma_{\phi} < H$) occurs in the midst of thermalization, in which case, the rate for that process never quite reaches the opposite edge of the band.
- [56] A. Boyarsky, A. Neronov, O. Ruchayskiy, and M. Shaposhnikov, Mon. Not. R. Astron. Soc. 370, 213 (2006).
- [57] S. Riemer-Sørensen, S. H. Hansen, and K. Pedersen, Astrophys. J. Lett. 644, L33 (2006).
- [58] M. Loewenstein, A. Kusenko, and P. L. Biermann, Astrophys. J. 700, 426 (2009).
- [59] C. R. Watson, Z.-Y. Li, and N. K. Polley, J. Cosmol. Astropart. Phys. 03 (2012) 018.
- [60] E. Borriello, M. Paolillo, G. Miele, G. Longo, and R. Owen, Mon. Not. R. Astron. Soc. 425, 1628 (2012).
- [61] S. Horiuchi, P. J. Humphrey, J. Onorbe, K. N. Abazajian, M. Kaplinghat, and S. Garrison-Kimmel, Phys. Rev. D 89, 025017 (2014).
- [62] T. Tamura, R. Iizuka, Y. Maeda, K. Mitsuda, and N. Y. Yamasaki, Publ. Astron. Soc. Jpn. 67, 23 (2015).
- [63] F. Hofmann, J. S. Sanders, K. Nandra, N. Clerc, and M. Gaspari, Astron. Astrophys. 592, A112 (2016).
- [64] F. Hofmann and C. Wegg, Astron. Astrophys. 625, L7 (2019).
- [65] J. W. Foster, M. Kongsore, C. Dessert, Y. Park, N. L. Rodd, K. Cranmer, and B. R. Safdi, Phys. Rev. Lett. 127, 051101 (2021).
- [66] K. Nandra et al., arXiv:1306.2307.
- [67] XRISM Science Team, arXiv:2003.04962.
- [68] F. A. Harrison et al., Astrophys. J. 770, 103 (2013).
- [69] S. Riemer-Sørensen et al., Astrophys. J. 810, 48 (2015).
- [70] K. Perez, K. C. Y. Ng, J. F. Beacom, C. Hersh, S. Horiuchi, and R. Krivonos, Phys. Rev. D 95, 123002 (2017).
- [71] K. C. Y. Ng, B. M. Roach, K. Perez, J. F. Beacom, S. Horiuchi, R. Krivonos, and D. R. Wik, Phys. Rev. D 99, 083005 (2019).
- [72] B. M. Roach, K. C. Y. Ng, K. Perez, J. F. Beacom, S. Horiuchi, R. Krivonos, and D. R. Wik, Phys. Rev. D 101, 103011 (2020).
- [73] B. M. Roach, S. Rossland, K. C. Y. Ng, K. Perez, J. F. Beacom, B. W. Grefenstette, S. Horiuchi, R. Krivonos, and D. R. Wik, Phys. Rev. D 107, 023009 (2023).
- [74] K. K. Madsen, J. A. García, D. Stern, R. Armini, S. Basso, D. Coutinho, B. W. Grefenstette, S. Kenyon, A. Moretti, P. Morrisey, K. Nandra, G. Pareschi, P. Predehl, A. Rau, D. Spiga, J. Willms, and W. W. Zhang, arXiv:2312.04678.
- [75] K. C. Y. Ng, S. Horiuchi, J. M. Gaskins, M. Smith, and R. Preece, Phys. Rev. D 92, 043503 (2015).

- [76] H. Yuksel, J. F. Beacom, and C. R. Watson, Phys. Rev. Lett. 101, 121301 (2008).
- [77] A. Boyarsky, D. Malyshev, A. Neronov, and O. Ruchayskiy, Mon. Not. R. Astron. Soc. 387, 1345 (2008).
- [78] G. M. Fuller, C. T. Kishimoto, and A. Kusenko, arXiv: 1110.6479.
- [79] E. O. Nadler, S. Birrer, D. Gilman, R. H. Wechsler, X. Du, A. Benson, A. M. Nierenberg, and T. Treu, Astrophys. J. 917, 7 (2021).
- [80] P. D. Bolton, F. F. Deppisch, and P. S. Bhupal Dev, J. High Energy Phys. 03 (2020) 170.
- [81] I. M. Shoemaker, K. Petraki, and A. Kusenko, J. High Energy Phys. 09 (2010) 060.
- [82] C. J. Martoff *et al.*, Quantum Sci. Technol. **6**, 024008 (2021).
- [83] S. Mertens et al. (KATRIN Collaboration), J. Phys. G 46, 065203 (2019).
- [84] M. Aker et al. (KATRIN Collaboration), Eur. Phys. J. C 83, 763 (2023).
- [85] C. Benso, V. Brdar, M. Lindner, and W. Rodejohann, Phys. Rev. D 100, 115035 (2019).
- [86] A. D. Dolgov, S. H. Hansen, G. Raffelt, and D. V. Semikoz, Nucl. Phys. **B590**, 562 (2000).
- [87] G. B. Gelmini, M. Kawasaki, A. Kusenko, K. Murai, and V. Takhistov, J. Cosmol. Astropart. Phys. 09 (2020) 051.
- [88] H. Rasmussen, A. McNichol, G.M. Fuller, and C.T. Kishimoto, Phys. Rev. D 105, 083513 (2022).
- [89] K. N. Abazajian and H. Garcia Escudero, Phys. Rev. D 108, 123036 (2023).
- [90] G. B. Gelmini, P. Lu, and V. Takhistov, J. Cosmol. Astropart. Phys. 06 (2020) 008.
- [91] G. B. Gelmini, P. Lu, and V. Takhistov, Phys. Lett. B 800, 135113 (2020).
- [92] G. B. Gelmini, P. Lu, and V. Takhistov, J. Cosmol. Astropart. Phys. 12 (2019) 047.
- [93] G. M. Fuller, A. Kusenko, and K. Petraki, Phys. Lett. B 670, 281 (2009).

- [94] G. Chauhan, S. Horiuchi, P. Huber, and I. M. Shoemaker, arXiv:2309.05860.
- [95] P. Carenza, G. Lucente, L. Mastrototaro, A. Mirizzi, and P. D. Serpico, Phys. Rev. D 109, 063010 (2024).
- [96] K. Akita, S. H. Im, M. Masud, and S. Yun, J. High Energy Phys. 07 (2024) 057.
- [97] J. Hidaka and G. M. Fuller, Phys. Rev. D **74**, 125015 (2006).
- [98] J. Hidaka and G. M. Fuller, Phys. Rev. D **76**, 083516 (2007).
- [99] C. A. Argüelles, V. Brdar, and J. Kopp, Phys. Rev. D 99, 043012 (2019).
- [100] A. M. Suliga, I. Tamborra, and M.-R. Wu, J. Cosmol. Astropart. Phys. 08 (2020) 018.
- [101] A. Ray and Y.-Z. Qian, Phys. Rev. D **108**, 063025 (2023).
- [102] D. N. Spergel and P. J. Steinhardt, Phys. Rev. Lett. 84, 3760 (2000).
- [103] M. Rocha, A. H. G. Peter, J. S. Bullock, M. Kaplinghat, S. Garrison-Kimmel, J. Onorbe, and L. A. Moustakas, Mon. Not. R. Astron. Soc. 430, 81 (2013).
- [104] S. Tulin and H.-B. Yu, Phys. Rep. 730, 1 (2018).
- [105] C. Garcia-Cely and X. Chu, arXiv:1705.06221.
- [106] N. E. Mavromatos, C. R. Argüelles, R. Ruffini, and J. A. Rueda, in 14th Marcel Grossmann Meeting on Recent Developments in Theoretical and Experimental General Relativity, Astrophysics, and Relativistic Field Theories (2017), Vol. 1, pp. 639–666, 10.1142/9789813226609_0035.
- [107] S. Adhikari et al., arXiv:2207.10638.
- [108] B. Moore, Nature (London) 370, 629 (1994).
- [109] S.-H. Oh, W. J. G. de Blok, F. Walter, E. Brinks, and R. C. Kennicutt, Jr, Astron. J. 136, 2761 (2008).
- [110] S.-H. Oh et al., Astron. J. 149, 180 (2015).
- [111] A. B. Balantekin, G. M. Fuller, A. Ray, and A. M. Suliga, Phys. Rev. D 108, 123011 (2023).